Investigating Polaron Transitions with Polar Molecules

Felipe Herrera, Kirk W. Madison, Roman V. Krems, and Mona Berciu

Phys. Rev. Lett. **110**, 223002 — Published 29 May 2013

DOI: 10.1103/PhysRevLett.110.223002

Investigating polaron transitions with polar molecules

Felipe Herrera,[1,2,3] Kirk W. Madison,[4] Roman V. Krems,[1] and Mona Berciu[4]

[1]*Department of Chemistry, University of British Columbia, Vancouver, B.C., V6T 1Z1, Canada*
[2]*Department of Chemistry, Purdue University, West Lafayette, IN 47907, USA*
[3]*Department of Chemistry and Chemical Biology, Harvard University, 12 Oxford St., Cambridge, MA 02138, USA*
[4]*Department of Physics and Astronomy, University of British Columbia, Vancouver, B.C., V6T 1Z1, Canada*

(Dated: March 25, 2013)

We determine the phase diagram of a polaron model with mixed breathing-mode and Su-Schrieffer-Heeger couplings and show that it has two sharp transitions, in contrast to pure models which exhibit one (for Su-Schrieffer-Heeger coupling) or no (for breathing-mode coupling) transition. We then show that ultracold molecules trapped in optical lattices can be used as a quantum simulator to study precisely this mixed Hamiltonian, and that the relative contributions of the two couplings can be tuned with external electric fields. The parameters of current experiments place them in the region where one of the transitions occurs. We also propose a scheme to measure the polaron dispersion using stimulated Raman spectroscopy.

PACS numbers: 34.50.Cx, 67.85.-d, 37.10.Gh, 37.10.De, 34.20.Cf, 52.55.Jd, 52.55.Lf, 37.10.Jk

Introduction: Polarons – the low-energy quasiparticles in the spectra of particles coupled to bosons – have been of broad interest in physics ever since Landau's first study [1]. There are two mechanisms for particle-boson coupling since bosons can change (i) the potential or (ii) the kinetic energy of the particle. For example, consider electron-phonon coupling. Vibrations of nearby atoms modulate the potential energy of an electron. Well-known examples of such type (i) interactions are the Holstein molecular crystal model [2] and the breathing-mode (BM) coupling relevant in cuprates [3]. At the same time, by modulating the distance between sites, phonons also affect the hopping integrals. Such effects are described by type (ii) models like the Su-Schrieffer-Heeger (SSH) or Peierls coupling, introduced for the study of conjugated polymers, *eg.* polyacetylene [4]. Many other examples of type (i) couplings (these are independent of the particle's momentum) and type (ii) couplings (these depend explicitly on the particle's momentum) appear in the study of carriers coupled to magnons and orbitons [5].

While *both* types of couplings are generally present, most early studies focused on type (i) models, in particular on the search for a self-trapping transition where the bosons create a potential well so deep that it traps the polaron. Type (i) models were shown to not exhibit such a transition [6], instead there is a smooth crossover from light, highly mobile polarons at weak coupling to heavy, small polarons at strong coupling. This standard view of the polaron as a quasiparticle that becomes heavier with increased coupling is now strongly challenged by results for type (ii) models. Recent work has shown that in such models the polaron can be lighter than the bare particle, since the bosons affect the particle's hopping so it may move more easily [7–9]. The boson-mediated dispersion is different from that of the bare particle and may favor a ground state with a different momentum [8]. If this happens, a sharp transition occurs when the boson-mediated contribution to the dispersion becomes dominant, as shown for the SSH polaron [9–11].

The different behaviour of type (i) and type (ii) polarons raises questions such as what is the behaviour in systems (cuprates [3], organic semiconductors [12]) where both types of couplings are important? What happens to the sharp transition in a mixed model if the coupling is varied smoothly from type (ii) to type (i)? This also makes it very desirable to find systems described by such mixed models but where, unlike in solid-state systems, all parameters can be tuned continuously. Quantum simulators using laser trapped atoms or molecules are particularly suited for this task. Interactions between particles at sub-mK temperatures can be tuned using laser fields to implement conditions that resemble those found in condensed matter [13]. Quantum simulators for type (i) lattice polarons have been proposed using atom-molecule systems [14], self-assembled crystals in strong DC fields [15], trapped ions [16] and Rydberg atoms [17]. The latter is also predicted to realize type (ii) couplings in the weak particle-boson interaction regime [18].

In this Letter we elucidate the polaron behavior as the coupling varies between type (ii) SSH and type (i) BM [19]. Surprisingly, we find that there are *two* sharp transitions, and that these occur even when the type (i) coupling is dominant. This shows that the polaron physics is much richer than generally assumed, and that type (ii) couplings may need to be included even for systems where they are usually neglected. We then show that this mixed Hamiltonian describes polar molecules trapped in an optical lattice, and moreover, that the parameters of current experiments place them in the region where a transition is expected to occur. Thus, experimental confirmation of such transitions is within reach. Furthermore, we propose a detection scheme equivalent to Angle-Resolved Photoemission Spectroscopy (ARPES) in solid-state systems [20] which directly measures the polaron dispersion and can pinpoint the transition.

Model: The generic single polaron Hamiltonian for a

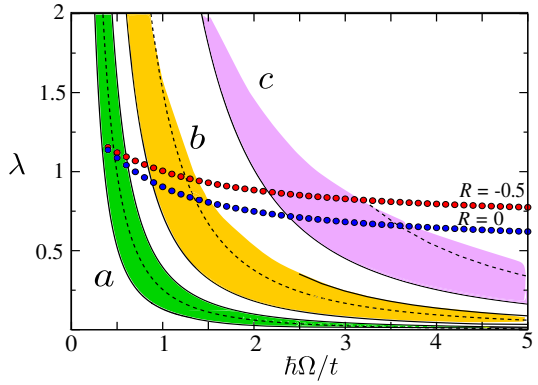

FIG. 1: (color online). Phase diagram λ vs. A at fixed R. Symbols show the location of the transition if $R = 0$ (blue circles) and $R = -0.5$ (red circles). The three shaded regions represent molecules with large (a, LiCs), intermediate (b, RbCs) and small (c, KRb) dipoles, and dressing schemes 1 ($R = -0.5$ for a) and 2 ($R = 0$ for b and c), respectively. For each region, the three lines correspond to lattice constants of 256 nm (lower bound), 532 nm (dashed line) and 775 nm (upper bound, not shown for region (c) because it is off-scale). For each curve $\hbar\Omega$ varies between 1 and 100 kHz.

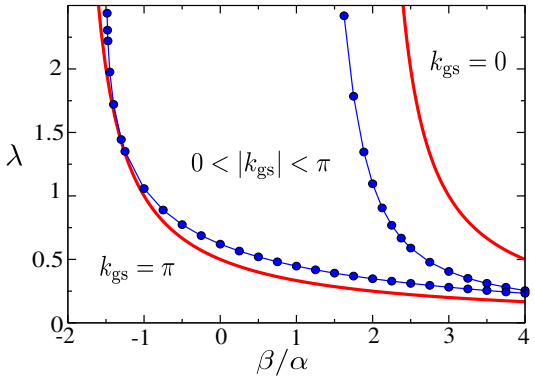

FIG. 2: (color online). Phase diagram λ vs. R at fixed A, showing two sharp transitions: one from a non-degenerate ground state with $k_{gs} = \pi$ to a doubly-degenerate ground state with $0 < |k_{gs}| < \pi$, and the second back to a non-degenerate ground state with $k_{gs} = 0$. The results are for $A = \hbar\Omega/t \to \infty$ (red lines) and for $A = 5$ (blue circles).

one-dimensional chain with N sites is:

$$\mathcal{H} = \sum_k \epsilon_k c_k^\dagger c_k + \sum_q \hbar\Omega_q b_q^\dagger b_q + \sum_{k,q} g_{k,q} c_{k+q}^\dagger c_k \left(b_{-q}^\dagger + b_q\right). \quad (1)$$

Here, c_k and b_q are annihilation operators for a particle with momentum k and a boson with momentum q, respectively. We assume a free particle dispersion $\epsilon_k = +2t\cos(k)$ with $t > 0$ [21] and Einstein bosons with $\Omega_q = \Omega$. The mixed SSH-BM coupling is given by:

$$g_{k,q} = \frac{2i}{\sqrt{N}} \left\{\alpha \left[\sin(k+q) - \sin(k)\right] + \beta \sin(q)\right\}. \quad (2)$$

The (k, q)-dependent part, with energy scale α, describes the type (ii) SSH coupling [9] while the k-independent part, with energy scale β, describes the type (i) BM coupling [19]. Following Ref. [9], we define the effective SSH coupling strength $\lambda = 2\alpha^2/(t\hbar\Omega)$ and the adiabaticity ratio $A = \hbar\Omega/t$. In addition, we use $R \equiv \beta/\alpha$ to characterize the relative strength of the two couplings.

The SSH polaron ($R = 0$) was predicted to undergo a sharp transition at a value λ^* [9]. Its physical origin is simple to understand in the anti-adiabatic limit $A \gg 1$ where the SSH coupling leads to an effective next-nearest neighbor hopping $i \leftrightarrow i+2$ of the particle, by first creating and then removing a boson at site $i+1$ [9]. Its amplitude is $t_2 = -\alpha^2/(\hbar\Omega) = -\lambda t/2 < 0$, so its contribution $-2t_2\cos(2k)$ to the total dispersion has a minimum at $\pi/2$, unlike the bare dispersion which has a minimum at π. If $4|t_2| = t$, corresponding to $\lambda^* = \frac{1}{2}$ in the limit of $A \gg 1$, a sharp transition marks the switch from a non-degenerate ground state with momentum $k_{gs} = \pi$ (for $\lambda < \lambda^*$) to a doubly-degenerate one with $|k_{gs}| \to \frac{\pi}{2}$ (for $\lambda > \lambda^*$). As A decreases the number of phonons in the polaron cloud increases. This renormalizes both hoppings $t \to t^*$, $t_2 \to t_2^*$, so λ^* changes smoothly with A as shown by the blue circles in Fig. 1 (see also Fig. 4 of Ref. [9]). We also plot λ^* for $R = -0.5$ (red circles), showing that the sharp polaron transition persists for coexisting type (i) and type (ii) couplings. These results were generated with the Momentum Average (MA) approximation, specifically its variational flavor where the polaron cloud is allowed to extend over any three consecutive sites [8, 9]. For $A \geq 0.3$, MA was shown to be very accurate for both SSH and BM couplings [9, 19].

To understand the evolution of λ^* with R, consider again the limit $A \gg 1$. In addition to the second-nearest neighbor hopping t_2, there is now also a dynamically generated nearest-neighbor hopping $t_1 = 2\alpha\beta/(\hbar\Omega) = R\lambda t$. This describes processes where the particle hops from site i to $i+1$ leaving behind a boson at i (SSH coupling) followed by absorption of the boson while the particle stays at $i+1$ (BM coupling); or vice versa, hence the factor of 2. The total nearest-neighbor hopping is thus $t^* = t - t_1$, and the transition now occurs when $4|t_2| = t^* \to \lambda^* = 1/(2+R)$. Thus, for $R < 0$, the interference between the SSH and the BM couplings results in a larger effective t^* leading to a larger λ^*. In particular, $\lambda^* \to \infty$ for $R \leq -2$, i.e. no transition occurs here. The lack of a transition is not surprising when $R \to -\infty$, since here the BM coupling is dominant and pure g_q models do not have transitions [6]. Our results show that for mixed SSH+BM coupling, the switch from having to not having a transition occurs abruptly at $R = -2$ if $A \gg 1$. This value must change continuously with A, therefore we expect this switch to always occur at a finite R.

This is confirmed in Fig. 2, where we plot λ^* vs. R for $A \to \infty$ and $A = 5$. Surprisingly, we find not just the transition at $\lambda^* \sim 1/(R+2)$, but also a second one which marks the crossing to a ground state with $k_{gs} = 0$. Its origin is also easy to understand in the anti-adiabatic

limit: if $R\lambda > 1$, t^* is negative and favors a ground state at $k_{\rm gs} = 0$ instead of $k_{\rm gs} = \pi$. For $A \gg 1$ this second transition is at $\lambda^* = 1/(R-2)$ if $R > 2$. At finite A, it moves towards smaller (R, λ) values, see Fig. 2.

Interestingly, this shows that for $R \to +\infty$ there are two nearby transitions for the shift $k_{gs} = \pi$ to $k_{\rm gs} = 0$. This seems to contradict the proof that a type-(i) Hamiltonian cannot have transitions [6], however, even for $R \to \infty$ this is a mixed Hamiltonian if $\lambda \neq 0$. The transition is indeed absent if $\alpha = 0$. This is an example of the rare occurrence where a perturbatively small term has a large effect on the behavior of the system.

Cold molecule implementation: Polar molecules in optical lattices can be used to implement Hamiltonian (1) in a wide region of the parameter space. Specifically, we consider molecules prepared in the ro-vibrational ground state of the spinless electronic state $^1\Sigma$ and trapped on an optical lattice in the Mott insulator phase, as recently demonstrated experimentally [22, 23]. We assume that there is at most one molecule per lattice site.

The dipole-dipole interaction between molecules in different sites can be modified by applying a DC electric field $\mathbf{E} = E_{\rm DC}\hat{\mathbf{z}}$ [15, 24–28]. Here we consider two schemes for dressing the rotational states of molecules with electric fields that are relevant for polaron observation, scheme 1 involving a DC electric field only, and scheme 2 involving combined optical and DC electric fields. For the former, we define the two-state subspace $|g\rangle = |\tilde{0}, 0\rangle$ and $|e\rangle = |\tilde{1}, 0\rangle$, where $|\tilde{N}, M_N\rangle$ denotes the field-dressed state that correlates adiabatically with the field-free rotational state $|N, M_N\rangle$. N is the rotational angular momentum and M_N is the projection of N along the electric field vector. In this basis we define the pseudospin operator $\hat{c}_i^\dagger \equiv |e_i\rangle\langle g_i|$ that creates a rotational excitation at site i. This excitation (the "bare particle") can be transferred between molecules in different lattice sites with an amplitude $t_{ij} = \gamma\, U_{ij}\,(1 - 3\cos^2\Theta)$, where $U_{ij} = d^2/|\mathbf{r}_i - \mathbf{r}_j|^3$, d is the permanent dipole moment, $\mathbf{r}_i$ is the position of molecule in site i, Θ is the polar angle of the intermolecular separation vector, $\gamma = \mu_{eg}^2/d^2 \leq 1$ is the dimensionless transition dipole moment that depends on the strength of the DC electric field. The excitation hopping amplitude is finite even for vanishing field strengths. The field-induced dipole-dipole interaction shifts the energy of the state $|e_i\rangle$ by $D_i = \sum_j D_{ij}$. Here $D_{ij} = -\kappa\, U_{ij}\,(1 - 3\cos^2\Theta)$, where $\kappa = |\mu_g(\mu_e - \mu_g)|/d^2$ and $\mu_g(\mu_e)$ is the induced dipole of the ground(excited) state. Dipolar couplings outside this two-level subspace are suppressed when the electric field separates state $|e\rangle$ from other excited states.

The free quasiparticle dispersion is $\epsilon_k = \varepsilon_0 + 2t\cos(k)$ where the site energy is $\varepsilon_0 = \hbar\omega_{eg} + D_0$, with the single-molecule rotational excitation energy $\hbar\omega_{eg} \sim 10$ GHz and $t \equiv t_{12}$. The center-of-mass vibration of molecules in the optical lattice potential is coupled to their internal rotation through the dependence of U_{ij} on $\mathbf{r}_i - \mathbf{r}_j$. For harmonic vibrations with linear coupling between internal and external degrees of freedom [15, 29], the boson term in Eq. (1) describes lattice phonons whose spectrum depends on the trapping laser intensity and the DC electric field [29]. Here we consider weak DC fields and moderate trapping frequencies which give a gapped and nearly dispersionless phonon spectrum with frequency Ω.

With these definitions, the system is described by SSH and BM-like couplings with the energy scales $\alpha = -3(t_{12}/a_L)\sqrt{\hbar/2m\Omega}$ and $\beta = -3(D_{12}/a_L)\sqrt{\hbar/2m\Omega}$, respectively, where m is the mass of the molecule and a_L is the lattice constant. The ratio $R = \beta/\alpha = \mu_g(\mu_e - \mu_g)/\mu_{eg}^2$ is independent of the intensity of the trapping laser or of the orientation of the array with respect to the DC field. In the field dressing scheme 1 we have $|R| < 1/2$ for $dE_{\rm DC}/B_e \leq 1$. In the combined AC-DC dressing scheme 2, the same DC field strength and orientation is used as above, but an additional two-color Raman coupling redefines the two-level subspace as $|g\rangle = \sqrt{a}\ |\tilde{0}, 0\rangle + \sqrt{1-a}\ |\tilde{2}, 0\rangle$ and $|e\rangle = \sqrt{b}\ |\tilde{1}, 0\rangle + \sqrt{1-b}\ |\tilde{3}, 0\rangle$ (details in the Supplementary Information). This dressing scheme can be used to effectively enhance the hopping amplitude by a factor $f > 1$ yielding $\alpha \to f\alpha$, without changing the value of β, nor the phonon dispersion. When using this dressing scheme, any point in the phase diagram transforms as $\lambda \to f\lambda$ and $A \to A/f$, thus shifting the system towards stronger SSH couplings.

The frequency of lattice phonons in a 1D array is $\Omega = (2/\hbar)\sqrt{V_0 E_R}$ where V_0 is the lattice depth and $E_R = \hbar^2\pi^2/2ma_L^2$ is the recoil energy. The particle-boson coupling can thus be written as $\lambda = 18(E_R/t)(\pi A)^{-2}$. The shaded regions in Fig. 1 show accessible points in the polaron phase diagram (λ, A) for LiCs, RbCs and KRb molecules, illustrating the flexibility in varying the Hamiltonian parameters when using the two field dressing scenarios and different experimental settings. Figure 1 shows that the transition characterized by the shift from a non-degenerate ground state $k_{\rm gs} = \pi$ to a degenerate ground state $0 < |k_{\rm gs}| < \pi$ can be studied using molecular species with moderate dipole moments such as RbCs, in lattices with a site separation $a_L \approx 500$ nm. However, the transition is easier to observe for molecules with large dipole moments such as LiRb and LiCs. For weakly dipolar molecules such as KRb, the strong coupling region can be achieved using $a_L < 500$ nm.

The most direct way to detect the transition is to measure the polaron dispersion. We propose the stimulated Raman spectroscopic scheme illustrated in Fig. 3 to achieve this goal. The one-dimensional array is initially prepared in the absolute ground state $|g\rangle = |g_1, \ldots, g_N\rangle|\{0\}\rangle$, where $|\{0\}\rangle$ is the phonon vacuum. We consider two linearly-polarized laser beams with wavevectors arranged such that $\mathbf{k}_1 - \mathbf{k}_2$ is parallel to the molecular array. If the laser beams are far-detuned from any vibronic resonance the effective light-matter interaction operator can be written as $\hat{V}(t) = -g_N[\hat{c}_q^\dagger e^{-i\omega t} + \hat{c}_q e^{i\omega t}]$, where g_N is a size-dependent coupling energy proportional to the amplitudes of both laser beams, $q = |\mathbf{k}_1 - \mathbf{k}_2|$ and $\omega = \omega_1 - \omega_2$ are the net momentum and energy trans-

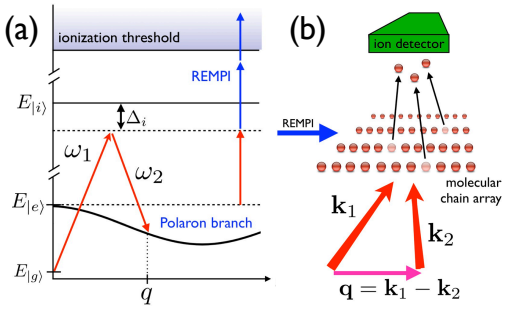

FIG. 3: (Color online) (a) A two-photon stimulated Raman transition creates a polaron state with a well defined momentum q and energy $\omega = \omega_1 - \omega_2$. (b) The presence of the quasiparticle is subsequently detected using resonantly-enhanced multi-photon ionization (REMPI).

ferred from the fields to the molecules. For short interaction times (linear response), the system is excited from $|g\rangle$ into the one-particle sector with a probability proportional to the spectral function $\mathcal{A}(q,\omega) = -\mathrm{Im}[G(q,\omega)]/\pi$ where $G(q,\omega) = \langle g|\hat{c}_q(\hbar\omega - \mathcal{H} + i\eta)^{-1}\hat{c}_q^\dagger|g\rangle$ is the one-particle Green's function. As a result, for any momentum q the polaron energy E_q equals the energy $\hbar\omega$ of the lowest-energy peak in $\mathcal{A}(q,\omega)$, in analogy with ARPES measurements [20].

To measure $\mathcal{A}(q,\omega)$, the stimulated Raman excitation rate can be determined using state selective resonance enhanced multi-photon ionization (REMPI), see Fig. 3(b). With some probability this converts the rotational excitation (the "particle") into a molecular ion which can be extracted from the chain and detected by a multichannel plate ion detector. Ionization and subsequent detection efficiencies for a 2 step REMPI processes can easily exceed 20% [30], and a properly gated integrator can resolve the arrival of a single molecular ion. Using a 3D lattice, a set of uncoupled parallel 1D arrays can be realized and excited simultaneously, increasing the signal to noise ratio of the detection step.

In summary, we have presented the first (to our knowledge) phase diagram for a mixed type polaron Hamiltonian [31], which showed that polaron physics is much richer than previously thought and that sharp transitions may occur even for dominantly type-(i) Hamiltonians ($R \gg 1$). We showed that polar molecules trapped in optical lattices can be used to study this physics, and proposed an ARPES-like detection scheme to directly measure the polaron dispersion and thus identify the transitions expected to occur in such systems [9, 11].

Many other aspects of single polaron physics can be investigated with trapped polar molecules, such as the effects of dispersive phonons (most theoretical work assumes Einstein bosons), or novel effects resulting from quadratic particle-boson coupling in the strong coupling regime, etc. Studying polaron phase diagrams in higher dimensions is easily achieved with the same experimental scheme. Generalizations to studies of bi-polarons are also of significant interest, to understand the pairing mechanism for dominantly type-(ii) models (to date most bi-polaron studies are for type-(i) models). Finally, one may also be able to adapt the polar molecules systems to study finite polaron concentrations. This would allow one to look for quantum phase transitions [32] and to study whether they can also be tuned by varying the particle-boson coupling.

Acknowledgements: Work supported by NSERC and CIFAR. FH would also like to thank NSF CCI center "Quantum Information for Quantum Chemistry (QIQC)", Award number CHE-1037992.

[1] L. D. Landau, Phys. Z. Sowjetunion **3**, 664 (1933).
[2] T. Holstein, Ann. Phys. (N.Y.) **8**, 325 (1959).
[3] O. Rösch and O. Gunnarson, Phys. Rev. Lett. **92**, 146403 (2004); B. Layo, M. Berciu and G. A. Sawatzky, Phys. Rev. B **76**, 174305 (2007); S. Johnston *et al.*, Phys. Rev. B **82**, 064513 (2010) and references therein.
[4] A. Heeger, S. Kivelson, J. R. Schrieffer and W. -P. Su, Rev. Mod. Phys. **60**, 781 (1988).
[5] for a small selection of such examples, see Z. Liu and E. Manousakis, Phys. Rev. B **45**, 2425 (1992); J. Bala *et al.*, Phys. Rev. Lett. **87**, 067204 (2001); A. S. Mishchenko and N. Nagaosa, Phys. Rev. Lett. **93**, 036402 (2004); A. Alvermann, D. M. Edwards, and H. Fehske, Phys. Rev. Lett. **98**, 056602 (2007); M. Daghofer *et al.*, Phys. Rev. Lett. **100**, 066403 (2008).
[6] B. Gerlach and H. Löwen, Rev. Mod. Phys. **63**, 63 (1991).
[7] A. Alvermann, D. M. Edwards, and H. Fehske, Phys. Rev. Lett. **98**, 056602 (2007).
[8] M. Berciu and H. Fehske, Phys. Rev. B **82**, 085116 (2010).
[9] D. J. J. Marchand *et al.*, Phys. Rev. Lett. **105**, 266605 (2010).
[10] K. Hannewald *et al.*, Phys. Rev. B **69**, 075211 (2004).
[11] V. M. Stojanović and M. Vanević, Phys. Rev. B **78**, 214301 (2008).
[12] Organic semiconductors where both type (i) and type (ii) couplings are important include BEDT-TTF, see A. Girlando *et al.*, Phys. Rev. B **66**, 100507(R) (2002); pentacene, see R. Hatch, D. Huber and H. Höchst, Phys. Rev. Lett. **104**, 047601 (2010); A. Girlando *et al.*, J. of Chem. Phys. **135**, 084701 (2011); rubrene, see A. Girlando *et al.*, Phys. Rev. B **82**, 035208 (2010); and other oligoacenes, see Ref. [10]; R. S. Sanchez-Carrera *et al.* J. Am. Chem. Soc. **132**, 14437 (2010); M. Casula, M. Calandra and F. Mauri, Phys. Rev. B **86** 075445 (2012).
[13] M. Lewenstein *et al.*, Adv. Phys. **56**, 243 (2007).
[14] M. Ortner *et al.*, New J. Phys. **11**, 055045 (2009).
[15] P. Rabl and P. Zoller, Phys. Rev. A. **76**, 042308 (2007).
[16] V. M. Stojanovic, T. Shi, C. Bruder and J. I. Cirac, Phys. Rev. Lett. **109**, 250501 (2012); A. Mezzacapo, J.

Casanova, L. Lamata, and E. Solano, Phys. Rev. Lett. **109**, 200501 (2012).
[17] J. P. Hague and C. MacCormick, Phys. Rev. Lett. **109**, 223001 (2012).
[18] J. P. Hague and C. MacCormick, New J. Phys. **14**, 033019 (2012).
[19] G. L. Goodvin and M. Berciu, Phys. Rev. B **23**, 235120 (2008).
[20] A. Damascelli, Z. Hussain, and Z.-X. Shen, Rev. Mod. Phys. **75**, 473 (2003).
[21] The results in Ref. [9] are for $t < 0$ in our sign convention. They can be mapped to $t > 0$ results by a unitary transformation that changes $k \to k + \pi$ and $R \to -R$. Length is measured in units of the lattice constant.
[22] C. Ospelkaus *et al.*, Phys. Rev. Lett. **97**, 120402 (2006).
[23] A. Chotia *et al.*, Phys. Rev. Lett. **108**, 080405 (2012).
[24] A. Micheli, G. K. Brennen and P. Zoller, Nat. Phys. **2**, 341 (2006).
[25] A. Micheli, G. Pupillo, H. P. Büchler and P. Zoller, Phys. Rev. A **76**, 043604 (2007).
[26] A. V. Gorshkov *et al.*, Phys. Rev. A. **84**, 033619 (2011).
[27] F. Herrera, M. Litinskaya and R. V. Krems, Phys. Rev. A **82**, 033428 (2010).
[28] J. P. Ríos, F. Herrera and R. V. Krems, New J. Phys. **12**, 103007 (2010).
[29] F. Herrera and R. V. Krems, Phys Rev. A. **84**, 051401(R) (2011).
[30] M. A. Bellos *et al.*, Phys. Chem. Chem. Phys. **13**, 18880 (2011).
[31] Results for the mixed Holstein + SSH coupling were presented in J. Sun, Y. Zhao, and W. Liang, Phys. Rev. B **79**, 155112 (2009) and, with addition of disorder, in S. Ciuchi and S. Fratini, Phys. Rev. Lett. **106**, 166403 (2011), however the existence of a transition is not discussed. Results for this mixed Hamiltonian in the adiabatic limit where phonons are treated semi-classically are presented in E. Piegari, C. A. Perroni, V. Cataudella, Eur. Phys. J. B **44**, 415 (2005) and C. A Perroni, V. Marigliano Ramaglia and V. Cataudella, Phys. Rev. B**84**, 014303 (2011).
[32] For a phase-diagram at half-filling in systems with type-(i) couplings, see M. Hohenadler, F. F. Assaad and H. Fehske, Phys. Rev. Lett. **109**, 116407 (2012) and references therein. For SSH coupling, a Peierls instability occurs at half-filling [4]. We are not aware of studies investigating mixed models at finite polaron concentrations.
[33] C. P. J. Adolphs and M. Berciu (unpublished).